Applications of image processing and machine learning to two non-invasive cancer diagnosis methods

Pablo Musé

pmuse@fing.edu.uy

Department of Signal Processing
Facultad de Ingeniería
Universidad de la República

March 16th, 2015

Motivation

Imaging and computer aided diagnosis have become an fundamental tool in medical practice. In this talk we present to examples that may end up being used in the near future:

1. Classification of pigmented skin lesions from dermoscopic images
   - In North America it is now the fifth most common cancer among males and the sixth most common cancer among females.
   - Early diagnosis and removal of thin melanoma is the most effective strategy. If diagnosed and treated early, the mean life expectancy can be increased by at least 25 years.
   - We achieve a specificity of 85% for a sensitivity of 90%.

2. Virtual colonoscopy and candidate polyp detection
   - Colorectal cancer: second leading cause of cancer-related deaths in the US and third worldwide.
   - Early detection of polyps reduces mortality rates up to 90%.
   - We achieve 100% sensitivity for polyps larger than 6 mm in size with just 0.9 false positives per case, and 93% sensitivity with 2.8 false positives per case for polyps larger than 3 mm in size.

Motivation

Imaging and computer aided diagnosis have become an fundamental tool in medical practice. In this talk we present to examples that may end up being used in the near future:

1. Classification of pigmented skin lesions from dermoscopic images
   - In North America it is now the fifth most common cancer among males and the sixth most common cancer among females.
   - Early diagnosis and removal of thin melanoma is the most effective strategy. If diagnosed and treated early, the mean life expectancy can be increased by at least 25 years.
   - We achieve a specificity of 85% for a sensitivity of 90%.

2. Virtual colonoscopy and candidate polyp detection
   - Colorectal cancer: second leading cause of cancer-related deaths in the US and third worldwide.
   - Early detection of polyps reduces mortality rates up to 90%.
   - We achieve 100% sensitivity for polyps larger than 6 mm in size with just 0.9 false positives per case, and 93% sensitivity with 2.8 false positives per case for polyps larger than 3 mm in size.

Motivation

Imaging and computer aided diagnosis have become an fundamental tool in medical practice. In this talk we present to examples that may end up being used in the near future:

1. Classification of pigmented skin lesions from dermoscopic images
   - In North America it is now the fifth most common cancer among males and the sixth most common cancer among females.
   - Early diagnosis and removal of thin melanoma is the most effective strategy. If diagnosed and treated early, the mean life expectancy can be increased by at least 25 years.
   - We achieve a specificity of 85% for a sensitivity of 90%.

2. Virtual colonoscopy and candidate polyp detection
   - Colorectal cancer: second leading cause of cancer-related deaths in the US and third worldwide.
   - Early detection of polyps reduces mortality rates up to 90%.
   - We achieve 100% sensitivity for polyps larger than 6 mm in size with just 0.9 false positives per case, and 93% sensitivity with 2.8 false positives per case for polyps larger than 3 mm in size.

Part 1: A tool to assist dermatologists in melanoma detection from dermoscopic images of pigmented skin lesions

G. Capdehourat, A. Corez, A. Bazzano, R. Alonso, P. Musé. *Toward a combined tool to assist dermatologists in melanoma detection from dermoscopic images of pigmented skin lesions*. Pattern Recognition Letters, 32(16), Dec. 2011.

What is dermoscopy?

Method to visualize submacroscopic morphology of pigmented lesions and identify structures localized deep in the epidermis.

- Image magnification and lighting system avoids reflection and refraction of cutaneous surface.
- Discovers pigment and vascular patterns, invisibles to the naked eye.
- Noninvasive, in vivo technique, very useful for melanoma diagnosis.

Commercial dermatoscopies

What is dermoscopy?

Method to visualize submacroscopic morphology of pigmented lesions and identify structures localized deep in the epidermis.

- Image magnification and lighting system avoids reflection and refraction of cutaneous surface.
- Discovers pigment and vascular patterns, invisibles to the naked eye.
- Noninvasive, in vivo technique, very useful for melanoma diagnosis.

Commercial dermatoscopies

Skin layers

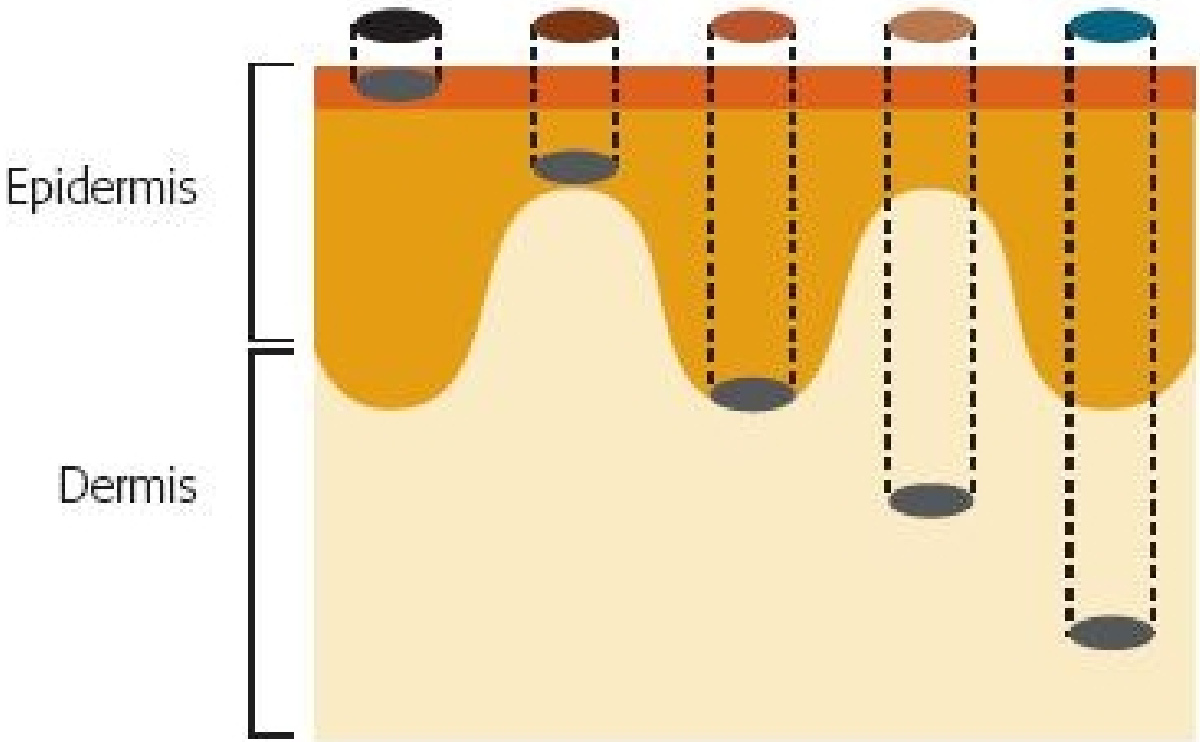

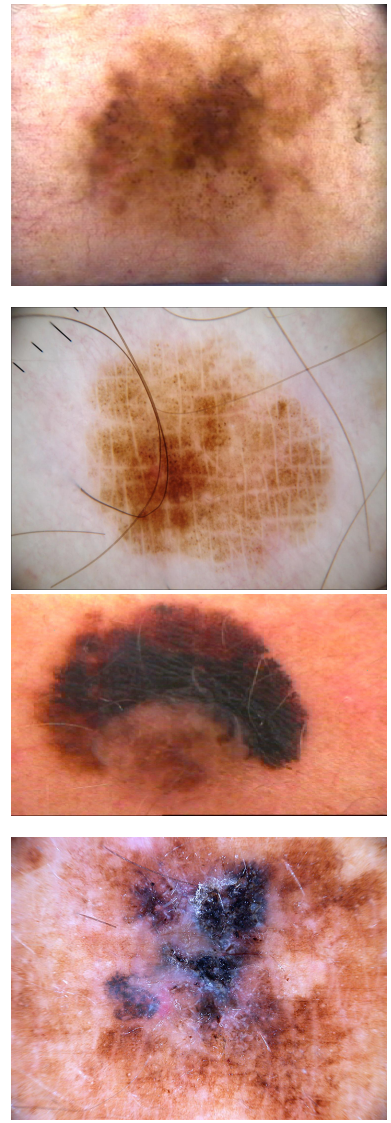

Melanocitic lesions structure

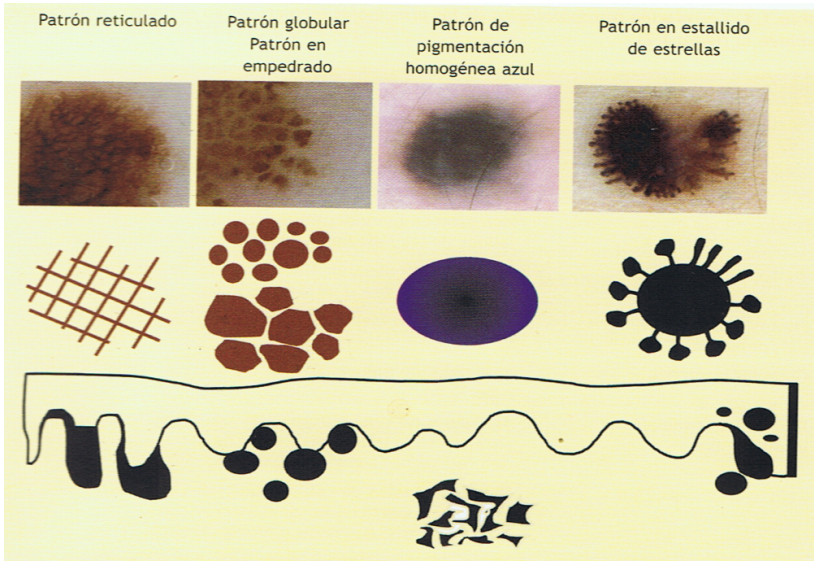

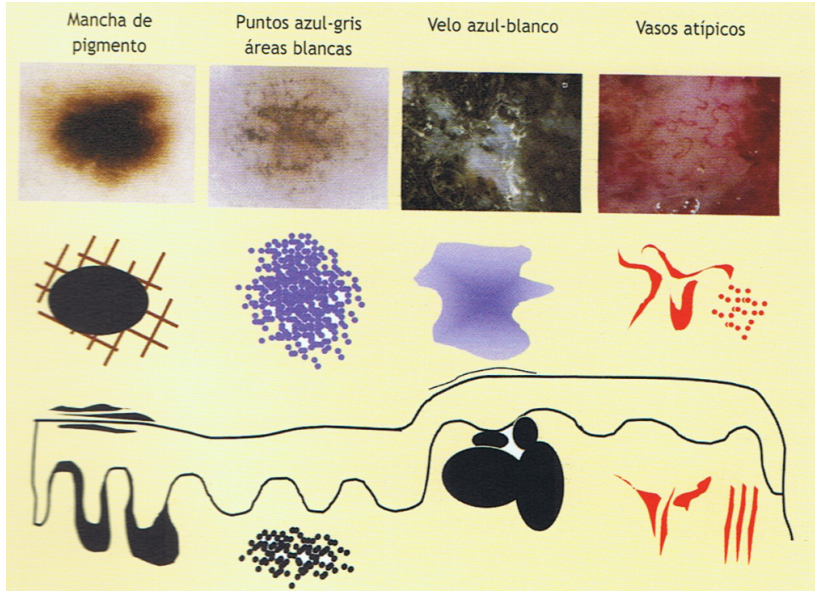

10-year survival rates as high as 99.5% for thin melanomas (smaller than 0.76mm Breslow index) compared to 48% for lesions larger than 3mm.

Only way to significantly reduce mortality: Early detection

Melanocitic lesions structure

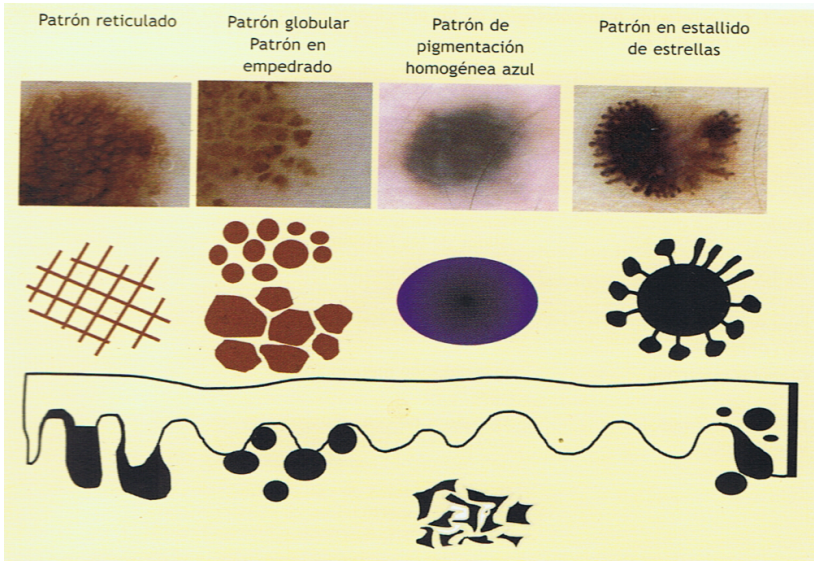

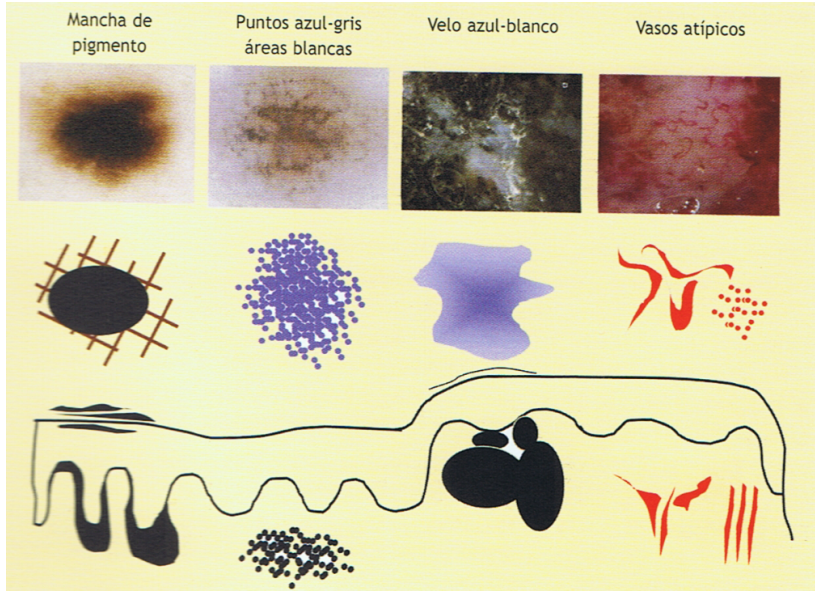

10-year survival rates as high as 99.5% for thin melanomas (smaller than 0.76mm Breslow index) compared to 48% for lesions larger than 3mm.

Only way to significantly reduce mortality: Early detection

Melanocitic lesions structure

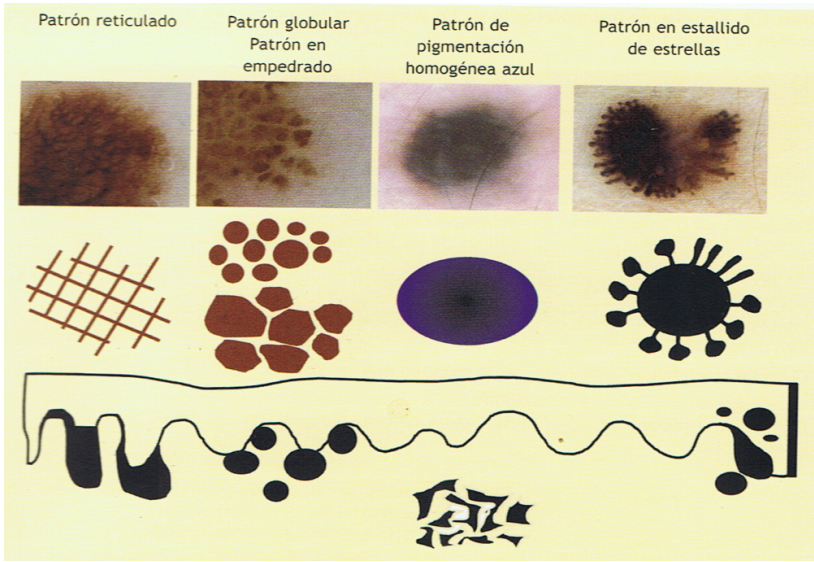

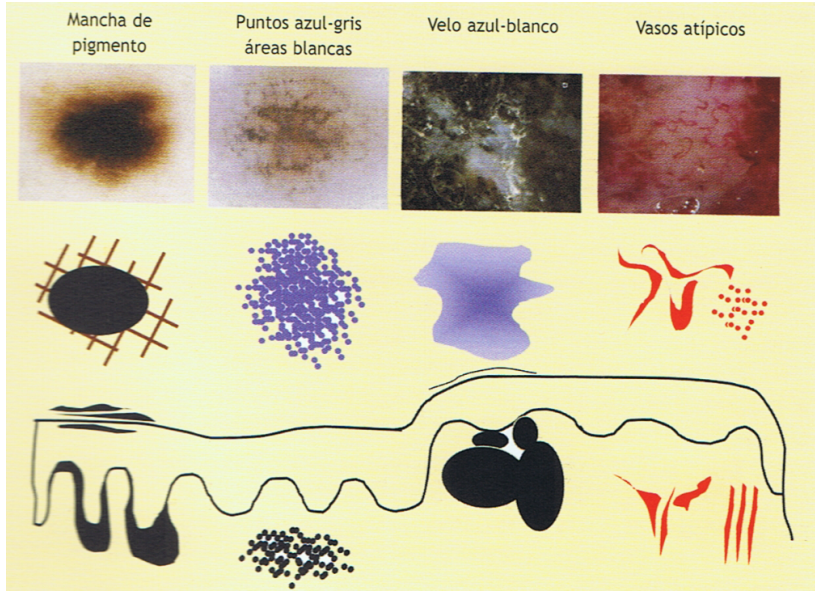

10-year survival rates as high as 99.5% for thin melanomas (smaller than 0.76mm Breslow index) compared to 48% for lesions larger than 3mm.

Only way to significantly reduce mortality: Early detection

Pigmented lesions classification

1st Step

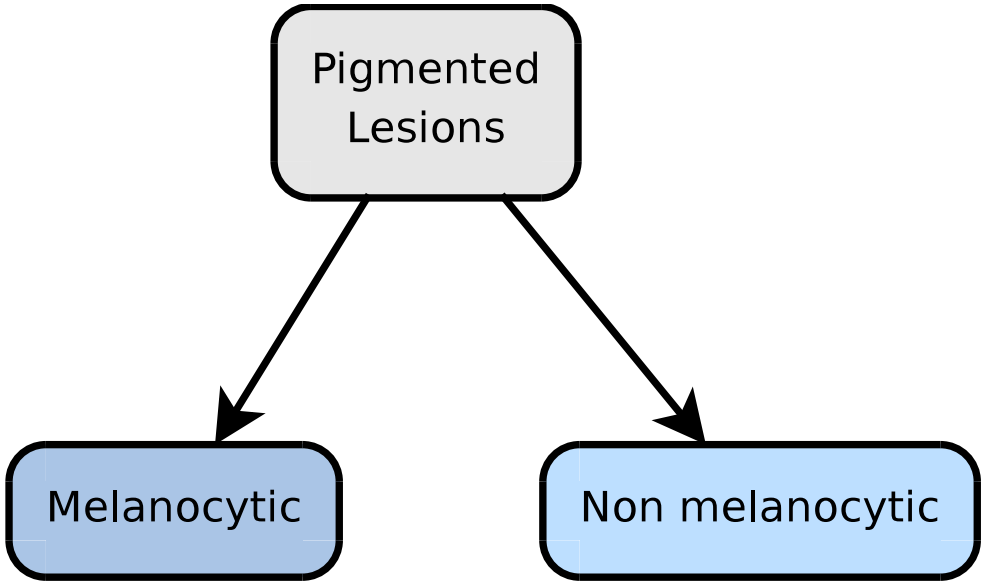

Pigmented lesions classification

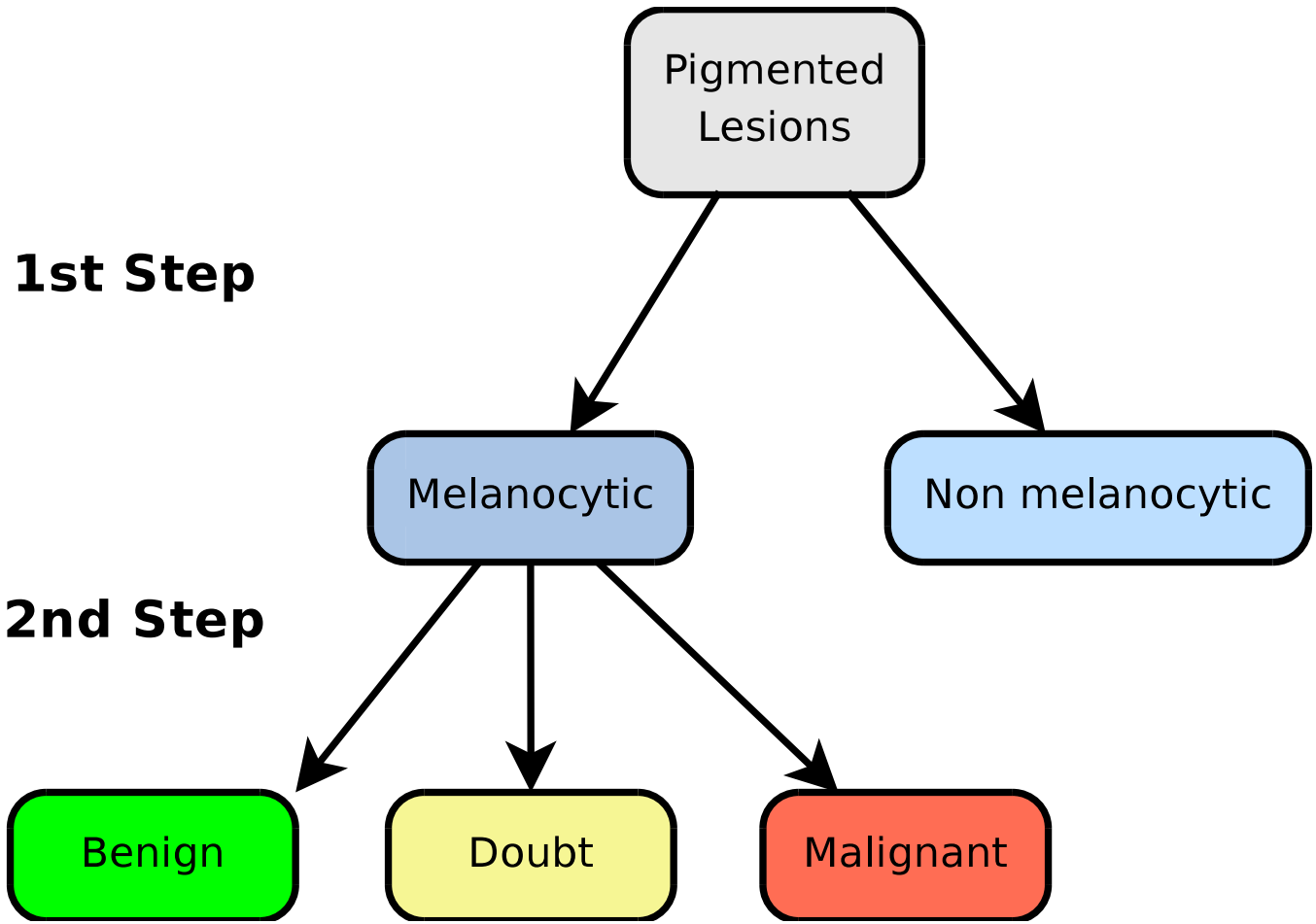

Pigmented lesions classification

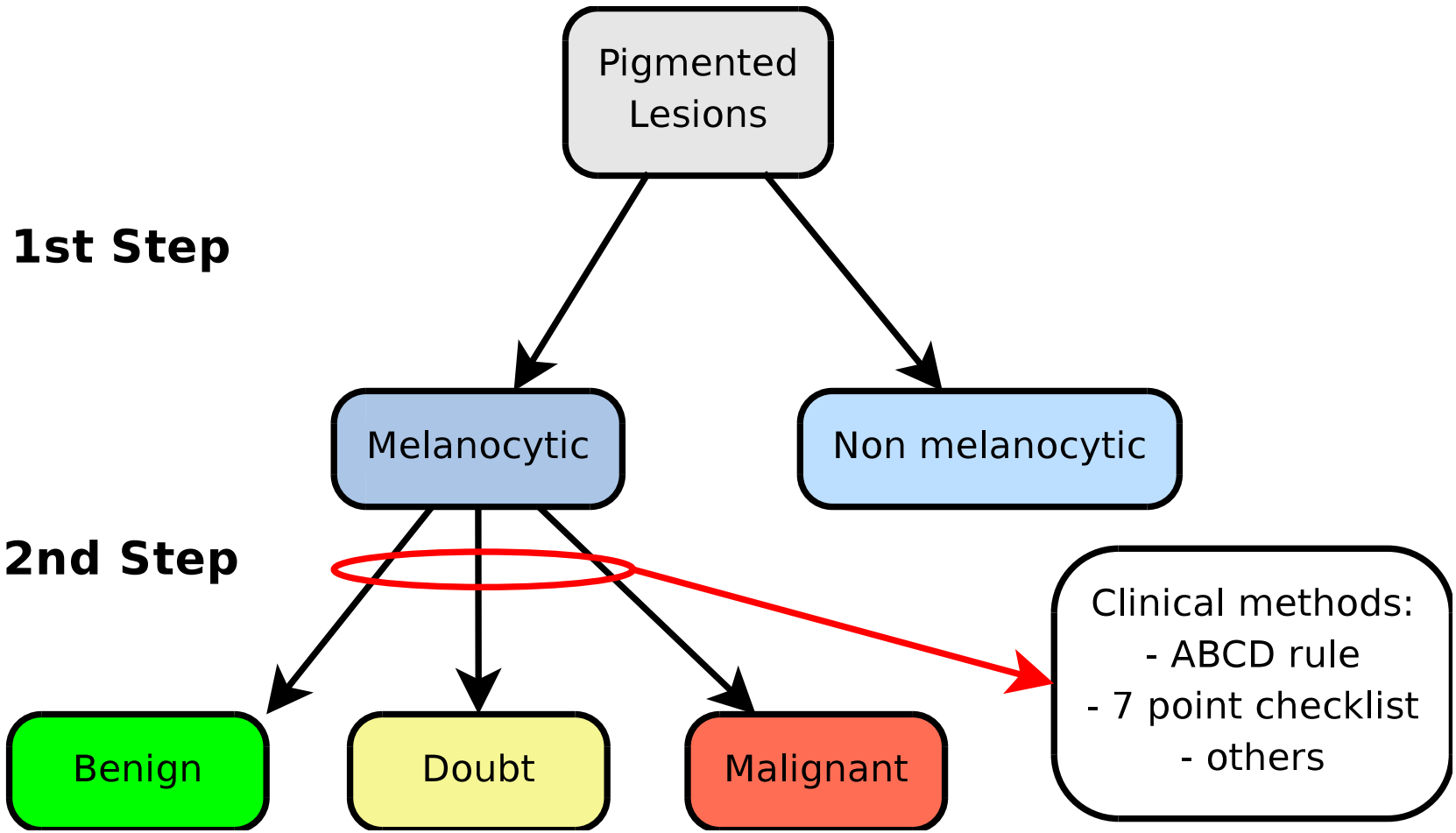

ABCD rule

Table V. Second-step algorithm: ABCD rule for the dermoscopic differentiation between benign melanocytic lesions and melanoma*

Dermoscopic criterion	Definition	Score	Weight factor
*A*symmetry	In 0, 1, or 2 perpendicular axes; assess not only contour, but also colors and structures	0-2	×1.3
*B*order	Abrupt ending of pigment pattern at periphery in 0-8 segments	0-8	×0.1
*C*olor	Presence of up to 6 colors (white, red, light-brown, dark-brown, blue-gray, black)	1-6	×0.5
*D*ermoscopic structures	Presence of network, structureless (homogeneous) areas, branched streaks, dots, and globules	1-5	×0.5

*Formula for calculating total score: [(A score × 1.3) + (B score × 0.1) + (C score × 0.5) + (D score × 0.5)]. Interpretation of total score: <4.75, benign melanocytic lesion; 4.75-5.45, suspect lesion (close follow-up or excision recommended); >5.45, lesion highly suspect for melanoma.

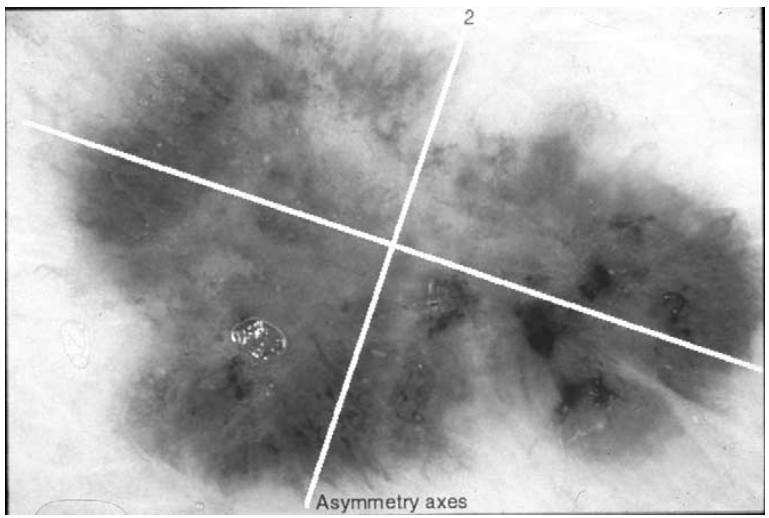

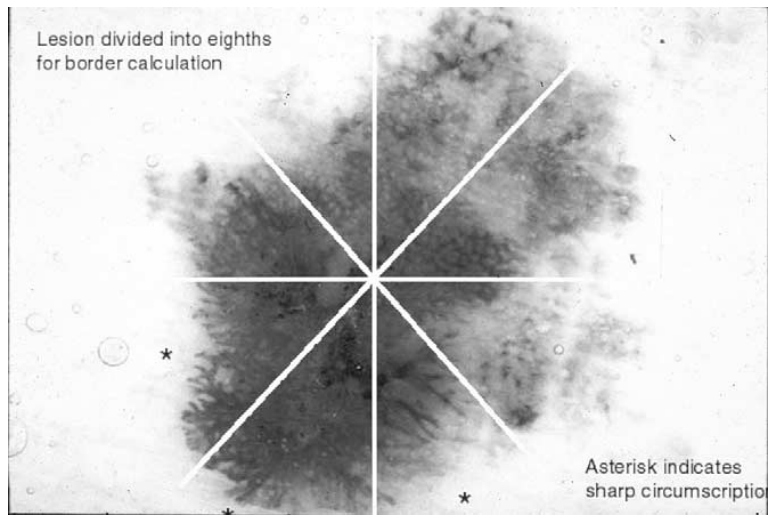

7 point checklist

Table 4. Seven-point checklist

Major criteria	*Points*
Atypical pigment network	2
Atypical vascular pattern	2
Blue-whitish veil	2
Minor criteria	
Irregular streaks (pseudopods/radial streaming)	1
Irregular pigmentation	1
Irregular dots/globules	1
Regression areas	1
Seven-point total score	
<3 = nonmelanoma	
≥3 = melanoma	

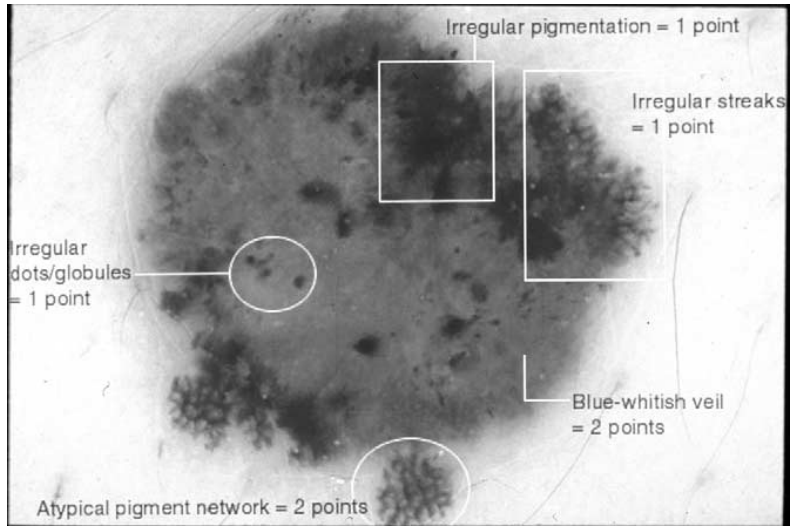

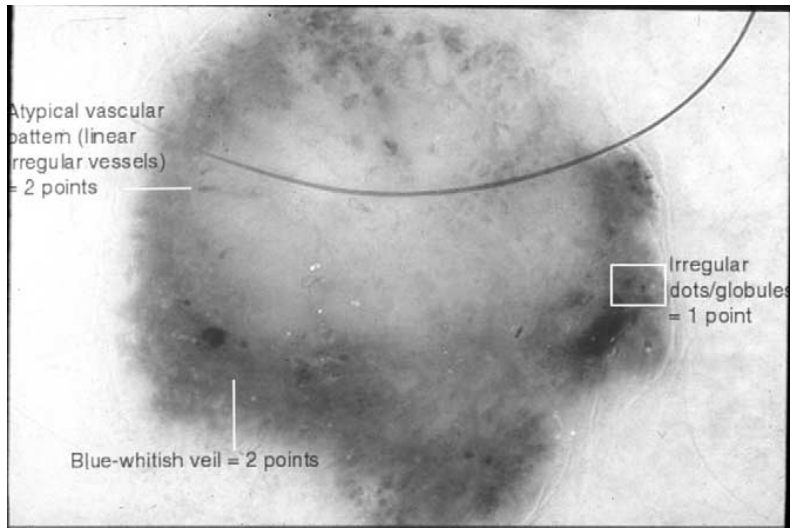

Clinical methods summary

- Several clinical methods available for melanoma diagnosis.
- None of them foolproof, all are complementary.
- No consensus in the medical community about which one to use.
- Training is very important, it depends on the doctor experience.
- Conclusion: it is always a subjective diagnosis.

An objective method can be helpful for screening campaigns, increasing the possibility of early diagnosis of melanoma.

Clinical methods summary

- Several clinical methods available for melanoma diagnosis.
- None of them foolproof, all are complementary.
- No consensus in the medical community about which one to use.
- Training is very important, it depends on the doctor experience.
- Conclusion: it is always a subjective diagnosis.

An objective method can be helpful for screening campaigns, increasing the possibility of early diagnosis of melanoma.

Method for automatic diagnosis

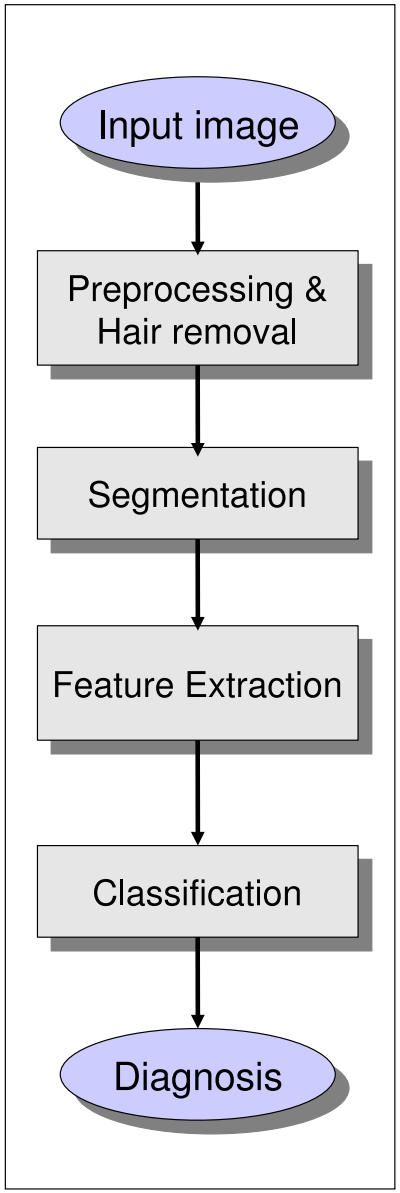

Computer aided image analysis in skin lesion diagnosis is a relatively new research field.

Previous work:

- 1st related work - *Cascinelli et al.* 1987.
- 1st significant contribution - *Gangster et al.* 2001.

  24-NN classifier
  Sensitivity=77% with specificity=84%.
- Best results found - *Celebi et al.* 2007.

  SVM classification
  Sensitivity=93.33% with specificity=92.34%.

Stages of our approach

Image preprocessing:

- Automatic hair removal based on *DullRazor* algorithm.
  - Hair detection:

    Discrete morphology with line structuring elements in several directions.

  - Image inpainting:

    Interpolation with nearby non-hair pixels in the normal direction.

- Image smoothing filter: median, mean, gaussian.

Image segmentation:

- Region based methods:
  - Otsu thresholding method.
  - Region based active contours.
- Border based methods:
  - Level line based methods.
  - Segmentation using the tree of shapes.

Stages of our approach

Image preprocessing:

- Automatic hair removal based on *DullRazor* algorithm.
  - Hair detection:

    Discrete morphology with line structuring elements in several directions.

  - Image inpainting:

    Interpolation with nearby non-hair pixels in the normal direction.
- Image smoothing filter: median, mean, gaussian.

Image segmentation:

- Region based methods:
  - Otsu thresholding method.
  - Region based active contours.
- Border based methods:
  - Level line based methods.
  - Segmentation using the tree of shapes.

Stages of our approach

Image preprocessing:

- Automatic hair removal based on *DullRazor* algorithm.
  - Hair detection:

    Discrete morphology with line structuring elements in several directions.

  - Image inpainting:

    Interpolation with nearby non-hair pixels in the normal direction.
- Image smoothing filter: median, mean, gaussian.

Image segmentation:

- Region based methods:
  - Otsu thresholding method.
  - Region based active contours.
- Border based methods:
  - Level line based methods.
  - Segmentation using the tree of shapes.

Preprocessing & segmentation results

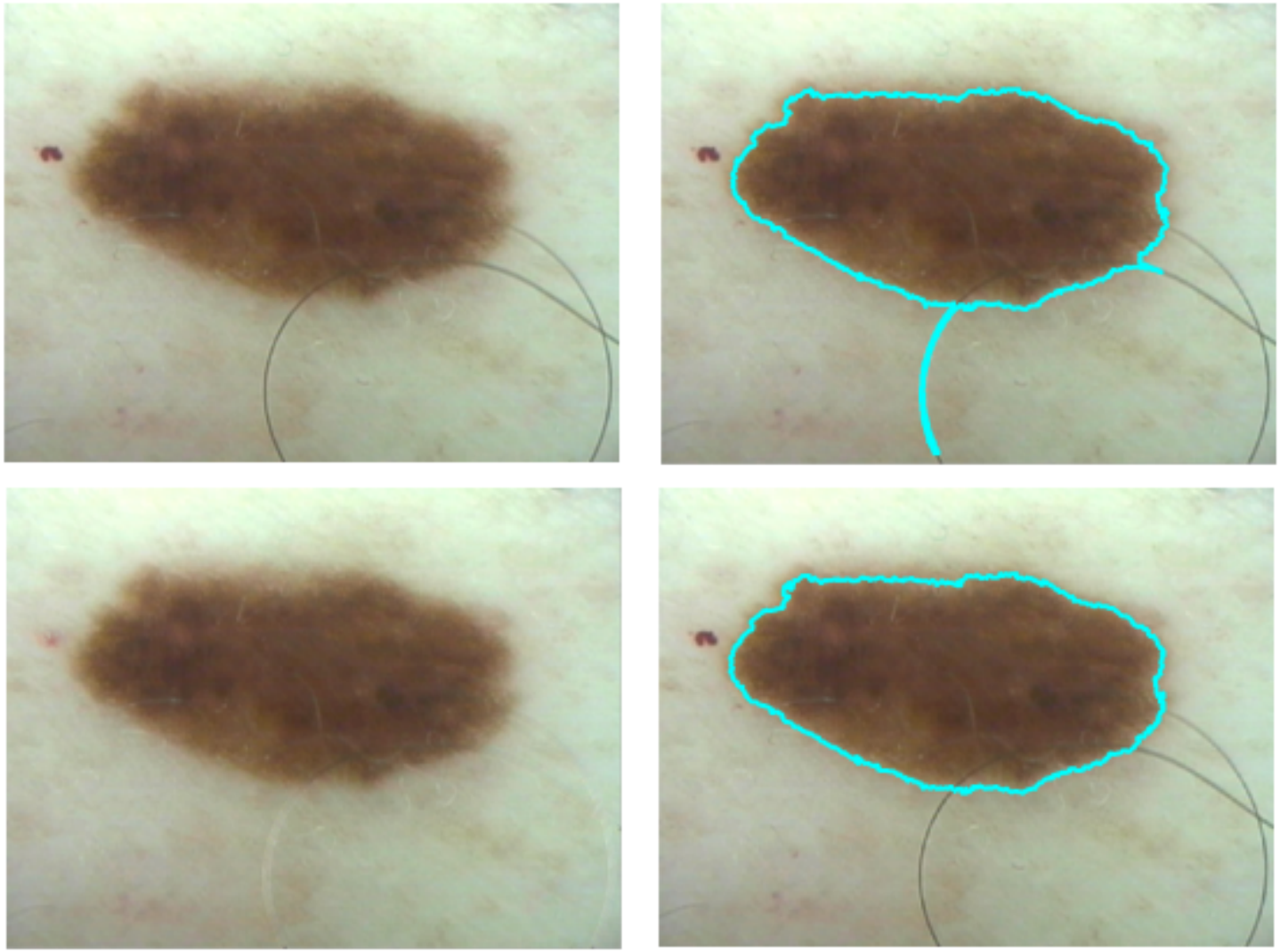

Preprocessing & segmentation results

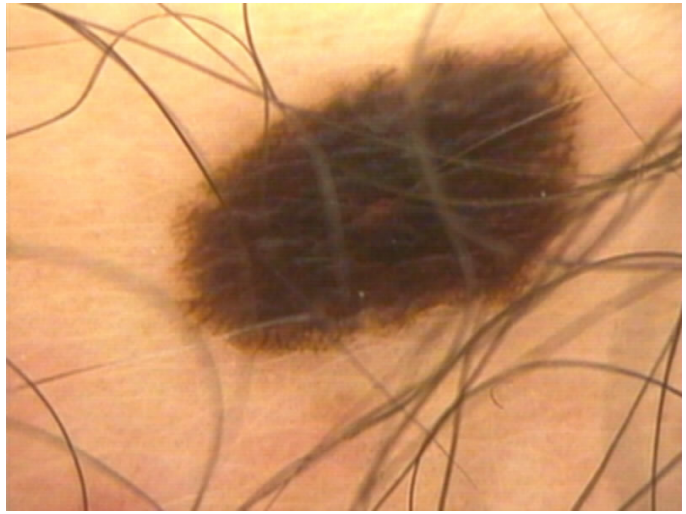

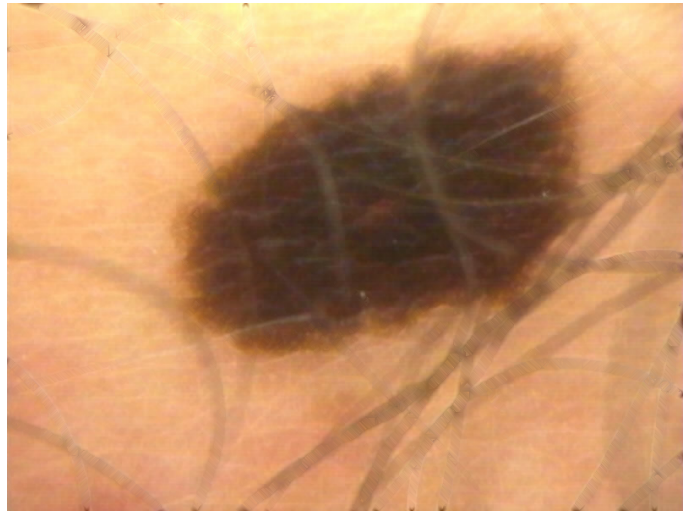

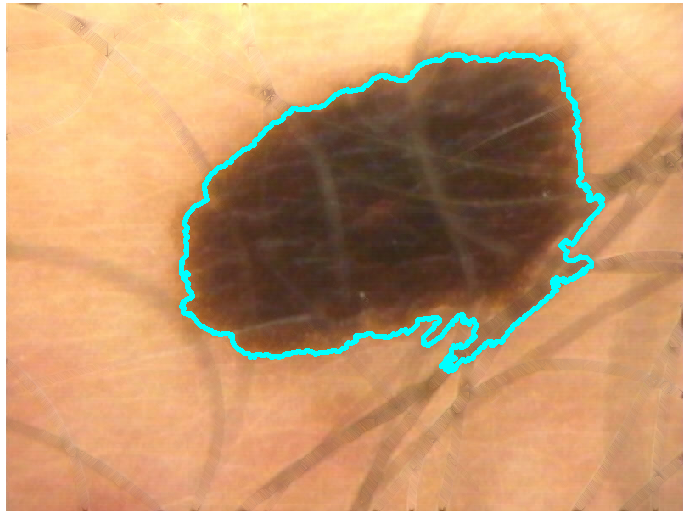

Feature extraction

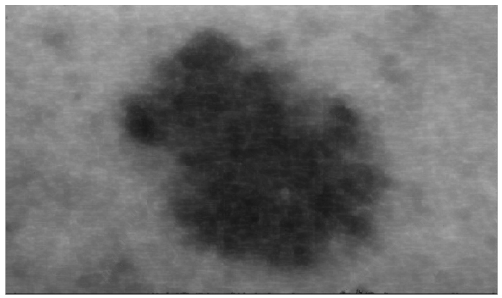

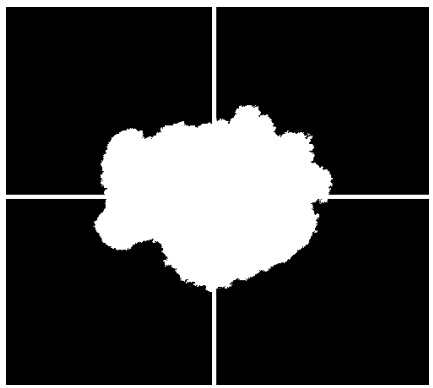

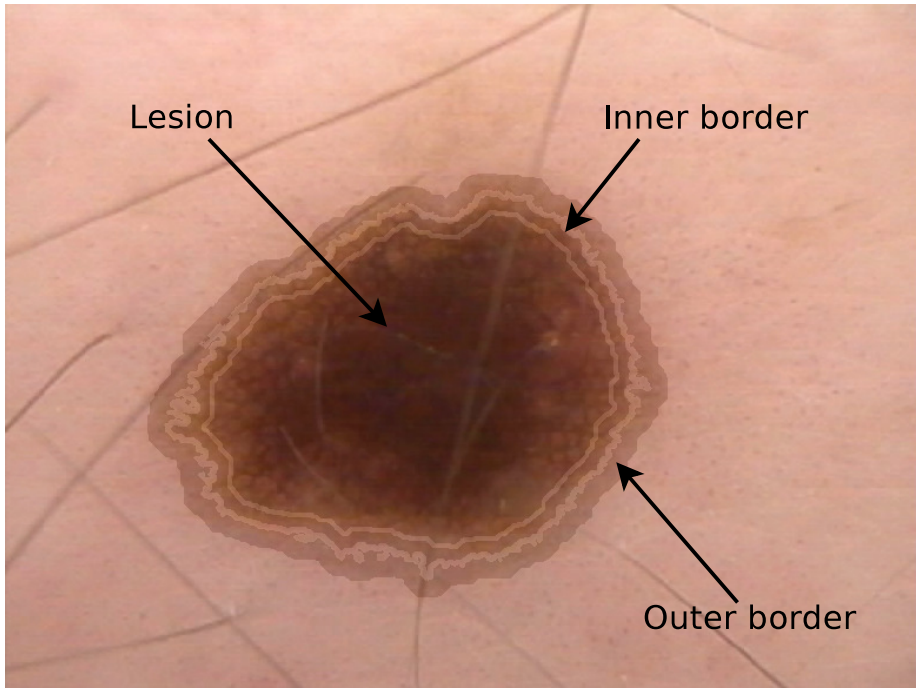

Chosen features are based on clinical methods of diagnosis:

- 7 shape features such as symmetry about both axes.
- 2 border features measuring lesion border hardness.
- 36 color features - $\mu \,\&\, \sigma$ for RGB & HSV for each 3 regions.
- 12 texture features - 4 statistics of GLCM[1] for each 3 regions.

[1] Gray-Level Co-occurrence Matrix

Training and classification

- Decision trees combination *via* adaptive boosting.
- Algorithm used: AdaBoost.M1 with C4.5 decision trees Weka implementation.
- Training procedure - optimization of AUC[2].
- Performance evaluation with 10 times 10-fold cross validation.
- Performance analysis:

  ROC curve: Sensibility vs. Specificity.

[2] area under the ROC curve

Database composition

- 513 images of melanocytic lesions: 433 benign and 80 malignant melanoma.
  - class imbalance problem dealt using sintetic resampling (SMOTE).
- Over a hundred correspond to dysplastic melanocytic nevi - visually the most alike to malignant melanoma.
- All of them have histopathologic studies, used as ground truth.
- Some images were discarded for the following reasons:
  - image do not capture the whole lesion.
  - poor image quality - blurred, low resolution.
  - excessive presence of hair.
- Every image has been manually segmented by a dermatologist.
- Diagnosis based on the ABCD rule and the 7-points checklist also provided.

System performance analysis

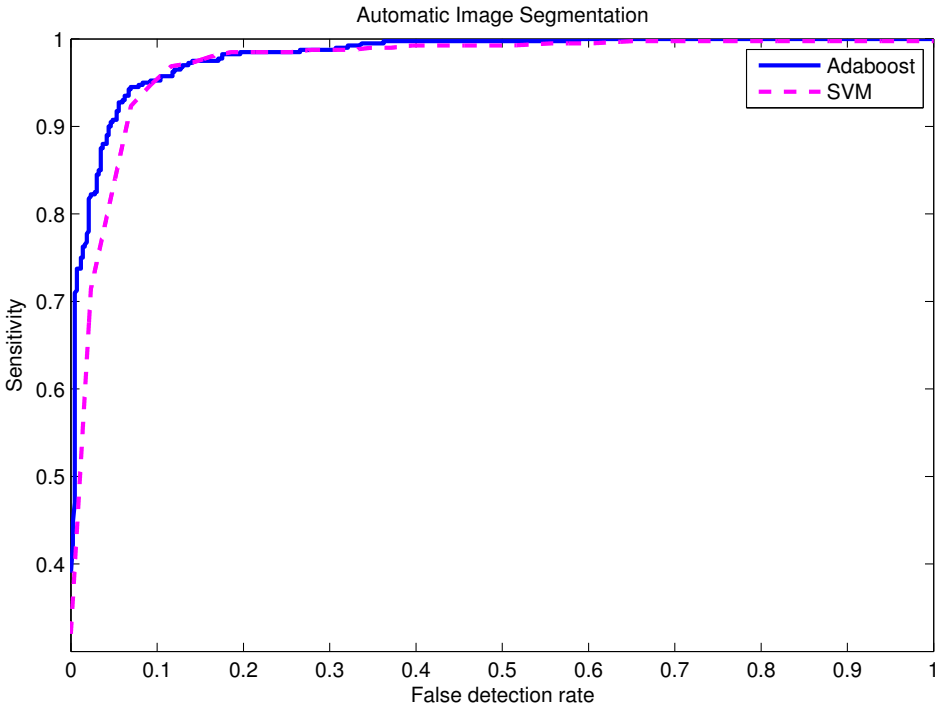

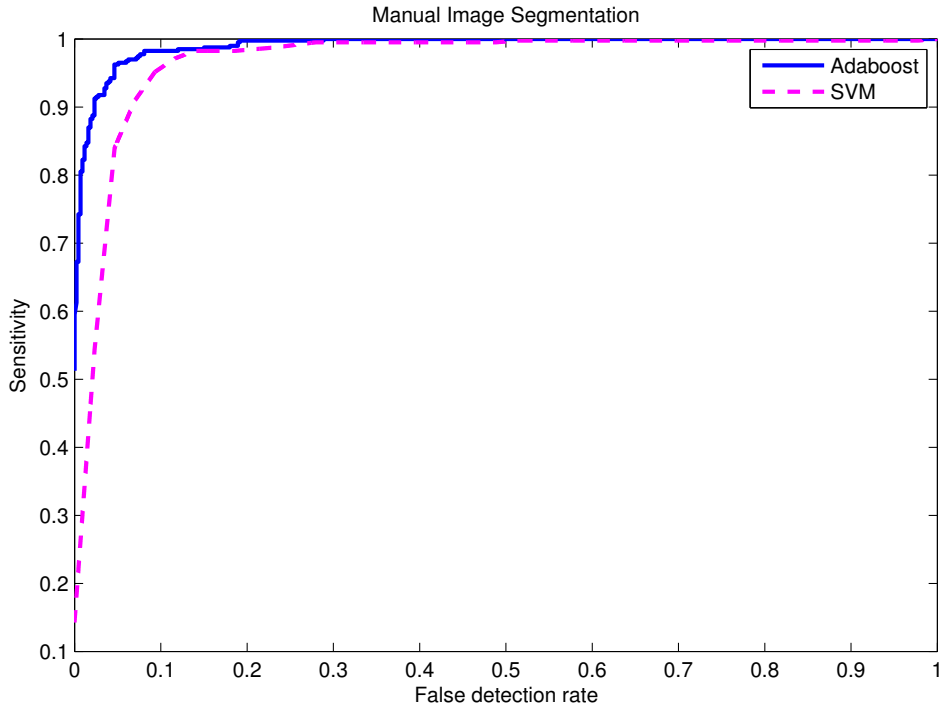

ROC curves for AdaBoost/C4.5 and SVM for automatic (L) and manual (R) segmentation.

Method	FPR for 95% sensitivity	Area under ROC
Automatic segmentation, AdaBoost - C4.5	8.75 %	0.981
Automatic segmentation, SVM	9.52 %	0.963
Manual segmentation, AdaBoost - C4.5	4.62%	0.991
Manual segmentation, SVM	9.23 %	0.966

Performance indicators for the ROC curves.

Comparison to previous work

- Database used by Celebi *et al.* is very similar in size and composition:
  - 476 benign lesions and 88 malignant melanoma.
- Results with SVM slightly better than those reported by Celebi *et al.*:
  - false positive rate of 14% for 95% sensitivity and AUC of 0.966.
- Our AdaBoost.M1 - C4.5 approach shows even higher performance.
  - false positive rate of 4.62% for 95% sensitivity and AUC of 0.991.

Comparison to previous work

- Database used by Celebi *et al.* is very similar in size and composition:
  - 476 benign lesions and 88 malignant melanoma.
- Results with SVM slightly better than those reported by Celebi *et al.*:
  - false positive rate of 14% for 95% sensitivity and AUC of 0.966.
- Our AdaBoost.M1 - C4.5 approach shows even higher performance.
  - false positive rate of 4.62% for 95% sensitivity and AUC of 0.991.

Comparison to previous work

- Database used by Celebi *et al.* is very similar in size and composition:
  - 476 benign lesions and 88 malignant melanoma.
- Results with SVM slightly better than those reported by Celebi *et al.*:
  - false positive rate of 14% for 95% sensitivity and AUC of 0.966.
- Our AdaBoost.M1 - C4.5 approach shows even higher performance.
  - false positive rate of 4.62% for 95% sensitivity and AUC of 0.991.

Misclassified lesions

False Negatives

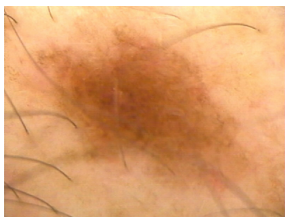

ABCD score=6
7 points=5

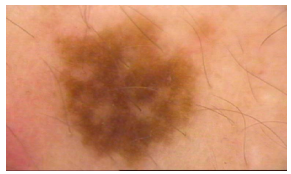

ABCD score=6.2
7 points=6

False Positives

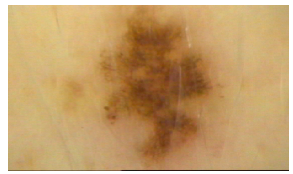

ABCD score=5
7 points=2

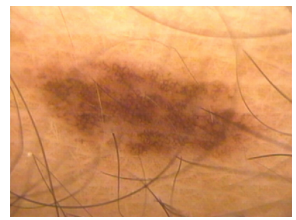

ABCD score=4.5
7 points=2

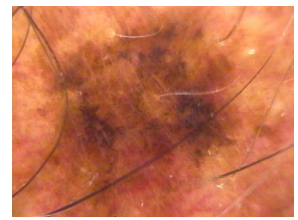

ABCD score=4.9
7 points=3

All misclassified patterns corresponding to lesion images.

- All false positives were dysplastic melanocytic nevi.
- Suspicious lesions according to the ABCD rule (scores from 4.75 to 5.45).
- False negatives posterior inspection - subjective overestimation of their scores.

Misclassified lesions

False Negatives

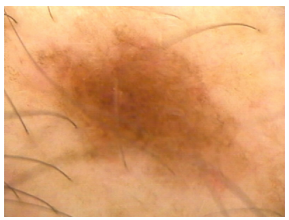

ABCD score=6
7 points=5

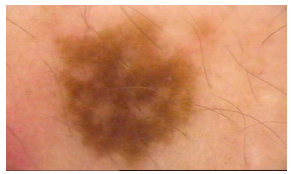

ABCD score=6.2
7 points=6

False Positives

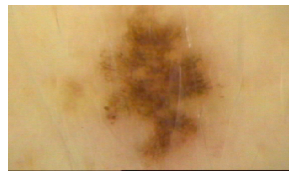

ABCD score=5
7 points=2

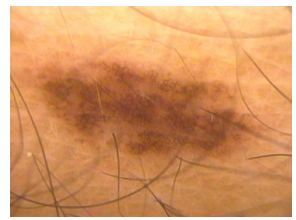

ABCD score=4.5
7 points=2

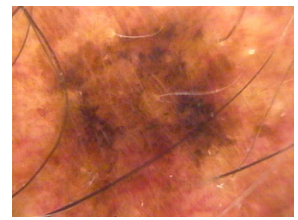

ABCD score=4.9
7 points=3

All misclassified patterns corresponding to lesion images.

- All false positives were dysplastic melanocytic nevi.
- Suspicious lesions according to the ABCD rule (scores from 4.75 to 5.45).
- False negatives posterior inspection - subjective overestimation of their scores.

Misclassified lesions

False Negatives

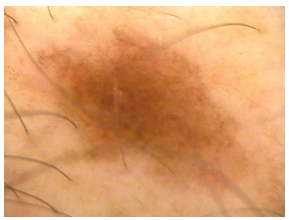

ABCD score=6
7 points=5

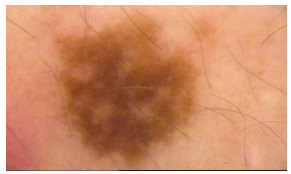

ABCD score=6.2
7 points=6

False Positives

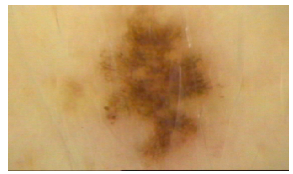

ABCD score=5
7 points=2

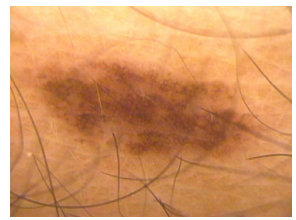

ABCD score=4.5
7 points=2

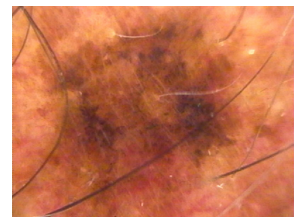

ABCD score=4.9
7 points=3

All misclassified patterns corresponding to lesion images.

- All false positives were dysplastic melanocytic nevi.
- Suspicious lesions according to the ABCD rule (scores from 4.75 to 5.45).
- False negatives posterior inspection - subjective overestimation of their scores.

Part 2: A Complete system for candidate polyps detection in virtual colonoscopy

M. Fiori, P. Musé, G. Sapiro. *A Complete system for candidate polyps detection in virtual colonoscopy.* Int. J. Patt. Recogn. Artif. Intell., 28(7), Nov. 2014.

Virtual Colonoscopy vs. Optical Colonoscopy

- Nowadays, optical colonoscopy (OC) is the most used detection method due in part to its high detection rate. However, this technique is invasive and expensive, making it hard to use in large screening campaigns.
- Virtual Colonoscopy (VC): promising alternative technique that emerged in the 90's. It uses volumetric Computed Tomographic data of the cleansed and air-distended colon.
- VC is less invasive than OC, and much more suitable for screening campaigns once its performance is demonstrated.
- In OC, incomplete studies due to obstructing lesions, colon twists, or anatomical variations are not rare (5% to 15% of OC examinations) and there is an additional important risk of colon perforation.

Virtual Colonoscopy vs. Optical Colonoscopy

- Nowadays, optical colonoscopy (OC) is the most used detection method due in part to its high detection rate. However, this technique is invasive and expensive, making it hard to use in large screening campaigns.
- Virtual Colonoscopy (VC): promising alternative technique that emerged in the 90's. It uses volumetric Computed Tomographic data of the cleansed and air-distended colon.
- VC is less invasive than OC, and much more suitable for screening campaigns once its performance is demonstrated.
- In OC, incomplete studies due to obstructing lesions, colon twists, or anatomical variations are not rare (5% to 15% of OC examinations) and there is an additional important risk of colon perforation.

Virtual Colonoscopy vs. Optical Colonoscopy

- Nowadays, optical colonoscopy (OC) is the most used detection method due in part to its high detection rate. However, this technique is invasive and expensive, making it hard to use in large screening campaigns.
- Virtual Colonoscopy (VC): promising alternative technique that emerged in the 90's. It uses volumetric Computed Tomographic data of the cleansed and air-distended colon.
- VC is less invasive than OC, and much more suitable for screening campaigns once its performance is demonstrated.
- In OC, incomplete studies due to obstructing lesions, colon twists, or anatomical variations are not rare (5% to 15% of OC examinations) and there is an additional important risk of colon perforation.

Goal of the present work

- Exploit VC precisely to automatically flag (mark for attention of the expert) colon regions with high probability of being polyps, with special attention to results in challenging small and flat polyps.
- Minimize the false negatives, keeping a reasonable false positives number.
- We achieve this by an automatic four-steps process that constitutes the entire end-to-end algorithm, from data to candidate polyps flagging.

Goal of the present work

- Exploit VC precisely to automatically flag (mark for attention of the expert) colon regions with high probability of being polyps, with special attention to results in challenging small and flat polyps.
- Minimize the false negatives, keeping a reasonable false positives number.
- We achieve this by an automatic four-steps process that constitutes the entire end-to-end algorithm, from data to candidate polyps flagging.

Goal of the present work

- Exploit VC precisely to automatically flag (mark for attention of the expert) colon regions with high probability of being polyps, with special attention to results in challenging small and flat polyps.
- Minimize the false negatives, keeping a reasonable false positives number.
- We achieve this by an automatic four-steps process that constitutes the entire end-to-end algorithm, from data to candidate polyps flagging.

Basic pipeline of the proposed polyp flagging system

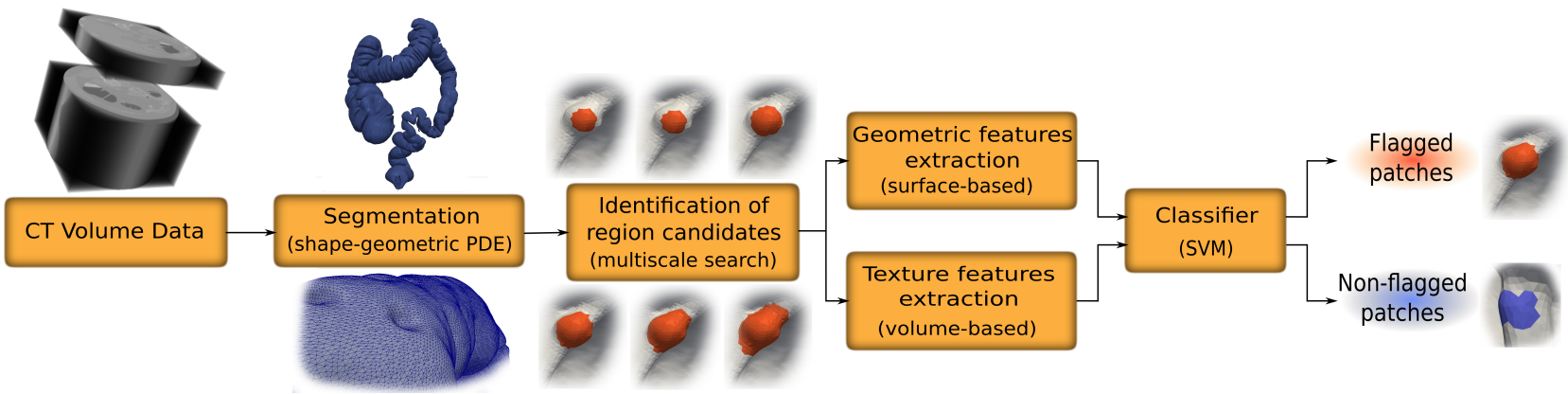

Remarks on previous work

- The main variations in the detection stage are in the features used and in the classification method.
- The most discriminant features are the geometric ones, and in particular curvature-based measures have been proved successful.
- All these techniques based on local geometric computations suffer from a high dependence on the regularity of the polyp shape itself, ignoring how pronounced it is with respect to the surrounding area.
- Using only geometry is also very sensitive to the accuracy of the segmentation.
- Texture features have been also used with promising results.
- To the best of our knowledge, no previous work reported in the literature can detect small polyps properly. On the other hand, for polyps larger than $6mm$ in size, no algorithm can achieve 100% sensitivity with less than one false positive per case.

Remarks on previous work

- The main variations in the detection stage are in the features used and in the classification method.
- The most discriminant features are the geometric ones, and in particular curvature-based measures have been proved successful.
- All these techniques based on local geometric computations suffer from a high dependence on the regularity of the polyp shape itself, ignoring how pronounced it is with respect to the surrounding area.
- Using only geometry is also very sensitive to the accuracy of the segmentation.
- Texture features have been also used with promising results.
- To the best of our knowledge, no previous work reported in the literature can detect small polyps properly. On the other hand, for polyps larger than $6mm$ in size, no algorithm can achieve 100% sensitivity with less than one false positive per case.

Remarks on previous work

- The main variations in the detection stage are in the features used and in the classification method.
- The most discriminant features are the geometric ones, and in particular curvature-based measures have been proved successful.
- All these techniques based on local geometric computations suffer from a high dependence on the regularity of the polyp shape itself, ignoring how pronounced it is with respect to the surrounding area.
- Using only geometry is also very sensitive to the accuracy of the segmentation.
- Texture features have been also used with promising results.
- To the best of our knowledge, no previous work reported in the literature can detect small polyps properly. On the other hand, for polyps larger than $6mm$ in size, no algorithm can achieve 100% sensitivity with less than one false positive per case.

Remarks on previous work

- The main variations in the detection stage are in the features used and in the classification method.
- The most discriminant features are the geometric ones, and in particular curvature-based measures have been proved successful.
- All these techniques based on local geometric computations suffer from a high dependence on the regularity of the polyp shape itself, ignoring how pronounced it is with respect to the surrounding area.
- Using only geometry is also very sensitive to the accuracy of the segmentation.
- Texture features have been also used with promising results.
- To the best of our knowledge, no previous work reported in the literature can detect small polyps properly. On the other hand, for polyps larger than $6mm$ in size, no algorithm can achieve 100% sensitivity with less than one false positive per case.

Remarks on previous work

- The main variations in the detection stage are in the features used and in the classification method.
- The most discriminant features are the geometric ones, and in particular curvature-based measures have been proved successful.
- All these techniques based on local geometric computations suffer from a high dependence on the regularity of the polyp shape itself, ignoring how pronounced it is with respect to the surrounding area.
- Using only geometry is also very sensitive to the accuracy of the segmentation.
- Texture features have been also used with promising results.
- To the best of our knowledge, no previous work reported in the literature can detect small polyps properly. On the other hand, for polyps larger than $6mm$ in size, no algorithm can achieve 100% sensitivity with less than one false positive per case.

Remarks on previous work

- The main variations in the detection stage are in the features used and in the classification method.
- The most discriminant features are the geometric ones, and in particular curvature-based measures have been proved successful.
- All these techniques based on local geometric computations suffer from a high dependence on the regularity of the polyp shape itself, ignoring how pronounced it is with respect to the surrounding area.
- Using only geometry is also very sensitive to the accuracy of the segmentation.
- Texture features have been also used with promising results.
- To the best of our knowledge, no previous work reported in the literature can detect small polyps properly. On the other hand, for polyps larger than $6mm$ in size, no algorithm can achieve 100% sensitivity with less than one false positive per case.

Remarks on previous work

- The main variations in the detection stage are in the features used and in the classification method.
- The most discriminant features are the geometric ones, and in particular curvature-based measures have been proved successful.
- All these techniques based on local geometric computations suffer from a high dependence on the regularity of the polyp shape itself, ignoring how pronounced it is with respect to the surrounding area.
- Using only geometry is also very sensitive to the accuracy of the segmentation.
- Texture features have been also used with promising results.
- To the best of our knowledge, no previous work reported in the literature can detect small polyps properly. On the other hand, for polyps larger than $6mm$ in size, no algorithm can achieve 100% sensitivity with less than one false positive per case.

1. Colon Segmentation: Two stages

1.1. Pre-processing: dealing with the air-fluid colon's composition.

Goal: compute a function u_0 intended to have homogeneous values in the colon interior and exterior, with smooth transition.

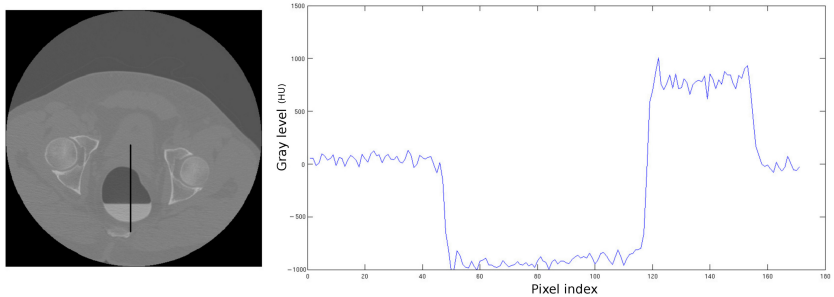

- At first sight: three clearly distinguishable classes.
- Nevertheless: six interface voxels between air and fluid whose gray values lie within the normal tissue range.
- It makes sense to assign to each voxel the likelihood of being air, fluid, or air-fluid interface. The air and fluid classification are performed by standard kernel density estimation techniques,
- This assignment fails on the air-fluid and air-fluid-tissue interfaces. **Solution:** The subject is laid horizontally so the voxels situated on the interface air-fluid have a large gradient in the vertical direction.

1. Colon Segmentation: Two stages

1.1. Pre-processing: dealing with the air-fluid colon's composition.

Goal: compute a function u_0 intended to have homogeneous values in the colon interior and exterior, with smooth transition.

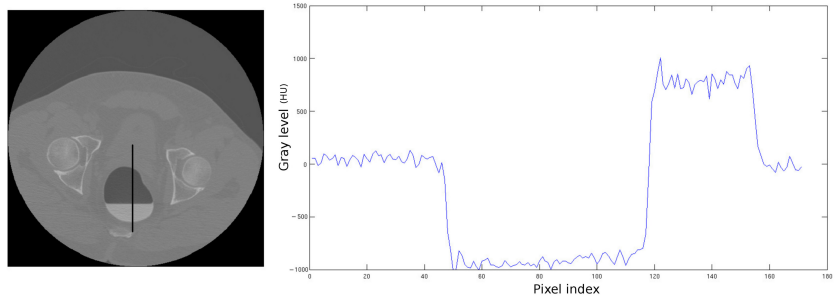

- At first sight: three clearly distinguishable classes.
- Nevertheless: six interface voxels between air and fluid whose gray values lie within the normal tissue range.
- It makes sense to assign to each voxel the likelihood of being air, fluid, or air-fluid interface. The air and fluid classification are performed by standard kernel density estimation techniques,
- This assignment fails on the air-fluid and air-fluid-tissue interfaces. **Solution:** The subject is laid horizontally so the voxels situated on the interface air-fluid have a large gradient in the vertical direction.

1. Colon Segmentation: Two stages

1.1. Pre-processing: dealing with the air-fluid colon's composition.

Goal: compute a function u_0 intended to have homogeneous values in the colon interior and exterior, with smooth transition.

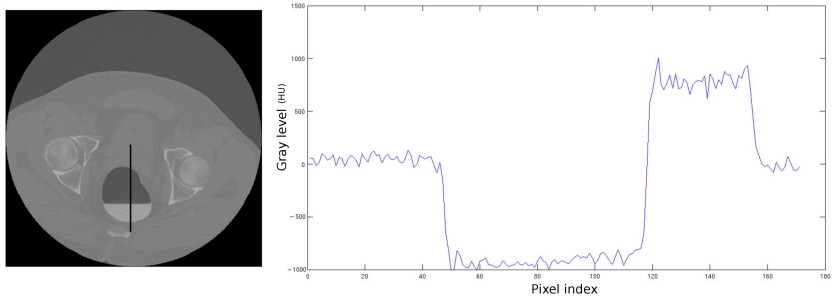

- At first sight: three clearly distinguishable classes.
- Nevertheless: six interface voxels between air and fluid whose gray values lie within the normal tissue range.
- It makes sense to assign to each voxel the likelihood of being air, fluid, or air-fluid interface. The air and fluid classification are performed by standard kernel density estimation techniques,
- This assignment fails on the air-fluid and air-fluid-tissue interfaces. **Solution:** The subject is laid horizontally so the voxels situated on the interface air-fluid have a large gradient in the vertical direction.

1. Colon Segmentation (cont.)

1.2. Smoothing the pre-processed volume u_0 to obtaining the final colon surface by as an iso-surface of the smoothed volume.

- We concentrate on a family of smoothing PDEs of the form

$$\frac{\partial u(\mathbf{x},t)}{\partial t} = \beta|\nabla u| \quad , \quad u(\mathbf{x},0) = u_0(\mathbf{x}).$$

  After a few iterations of this evolution, the inner colonic wall will be extracted as a suitable iso-level surface of the resulting $3D$ image $u(\mathbf{x},T)$.
- The Level Sets Method states that if $u(\mathbf{x},t)$ evolves according to the former equation, then its iso-levels (level sets) satisfy $\frac{\partial \mathcal{S}}{\partial t} = \beta\vec{\mathcal{N}}$, where $\mathcal{S}$ is any iso-level surface and $\vec{\mathcal{N}}$ its unit normal. This geometric view enables to design β to fulfill a set of requirements we will impose to the surface evolution. In particular, we are interested in motions driven by the principal curvatures. **(LATER)**

1. Colon Segmentation (cont.)

1.2. Smoothing the pre-processed volume u_0 to obtaining the final colon surface by as an iso-surface of the smoothed volume.

- We concentrate on a family of smoothing PDEs of the form

$$\frac{\partial u(\mathbf{x},t)}{\partial t} = \beta|\nabla u| \quad , \quad u(\mathbf{x},0) = u_0(\mathbf{x}).$$

  After a few iterations of this evolution, the inner colonic wall will be extracted as a suitable iso-level surface of the resulting $3D$ image $u(\mathbf{x},T)$.

- The Level Sets Method states that if $u(\mathbf{x},t)$ evolves according to the former equation, then its iso-levels (level sets) satisfy $\frac{\partial \mathcal{S}}{\partial t} = \beta\vec{\mathcal{N}}$, where $\mathcal{S}$ is any iso-level surface and $\vec{\mathcal{N}}$ its unit normal. This geometric view enables to design β to fulfill a set of requirements we will impose to the surface evolution. In particular, we are interested in motions driven by the principal curvatures. **(LATER)**

1. Colon Segmentation (cont.)

1.2. Smoothing the pre-processed volume u_0 to obtaining the final colon surface by as an iso-surface of the smoothed volume.

- We concentrate on a family of smoothing PDEs of the form

$$\frac{\partial u(\mathbf{x},t)}{\partial t} = \beta|\nabla u| \quad , \quad u(\mathbf{x},0) = u_0(\mathbf{x}).$$

  After a few iterations of this evolution, the inner colonic wall will be extracted as a suitable iso-level surface of the resulting $3D$ image $u(\mathbf{x},T)$.

- The Level Sets Method states that if $u(\mathbf{x},t)$ evolves according to the former equation, then its iso-levels (level sets) satisfy $\frac{\partial \mathcal{S}}{\partial t} = \beta\vec{\mathcal{N}}$, where $\mathcal{S}$ is any iso-level surface and $\vec{\mathcal{N}}$ its unit normal. This geometric view enables to design β to fulfill a set of requirements we will impose to the surface evolution. In particular, we are interested in motions driven by the principal curvatures. **(LATER)**

2. Feature extraction

Introducing "differential" features: It is important to analyze the spatial context in which the candidate patch is located, mainly because polyps can be situated over different structures such as folds or plain colonic wall. **A good feature including the shape of the neighborhood for example, can help in the discrimination between irregular folds and polyps over folds.**

Surfaces for geometric features

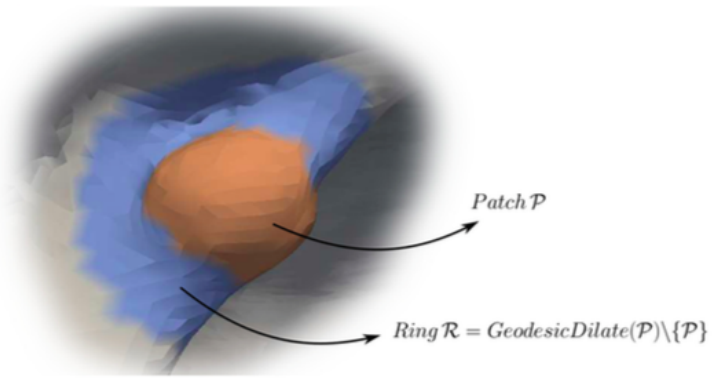

Volumes for texture features

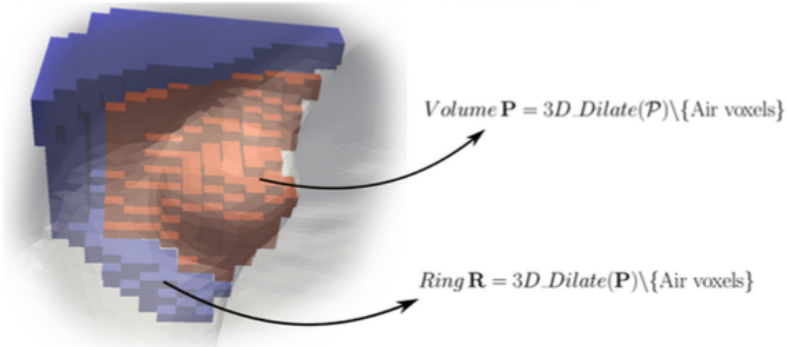

2.1. Feature extraction: Geometric features

- *Shape Index S*:

$$S := -\frac{2}{\pi}\arctan\left(\frac{\kappa_{max}+\kappa_{min}}{\kappa_{max}-\kappa_{min}}\right)$$

- *Curvedness C*:

$$R := \sqrt{\frac{\kappa_{max}^2+\kappa_{min}^2}{2}} \quad , \quad C := \frac{2}{\pi}\ln R$$

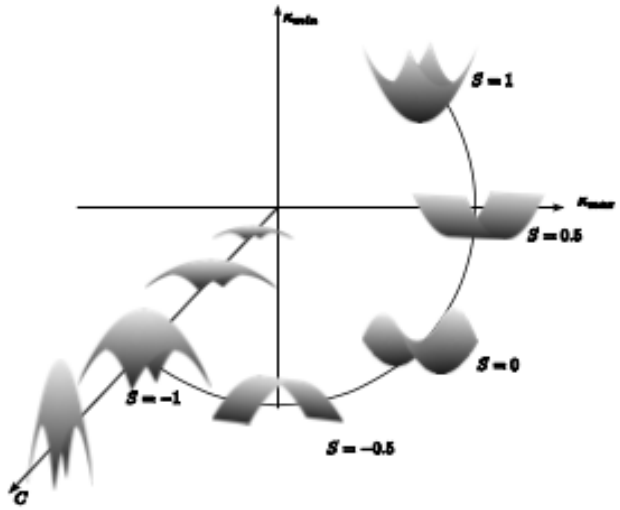

- 6 geometric features:

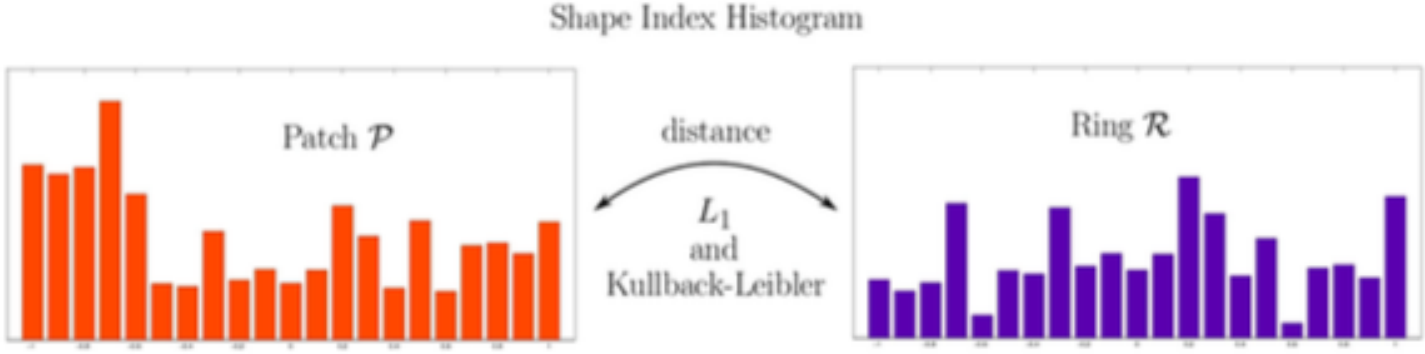

- 3 mean values of Shape Index computed with different Gaussian filters.
- Shape Factor: $SF := \frac{4\pi \cdot Area}{Perimeter^2}$

2.2. Feature extraction: Texture features

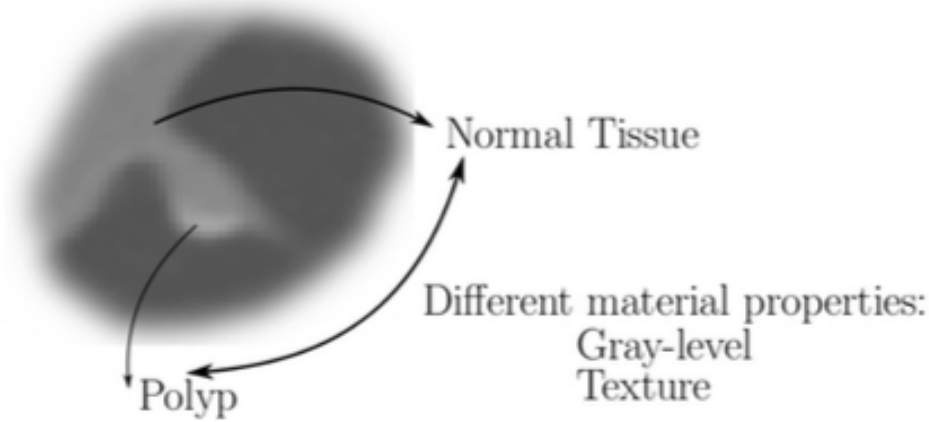

- Normal tissue properties may vary with its location in the colon.
  $\Rightarrow$ Use differential features!

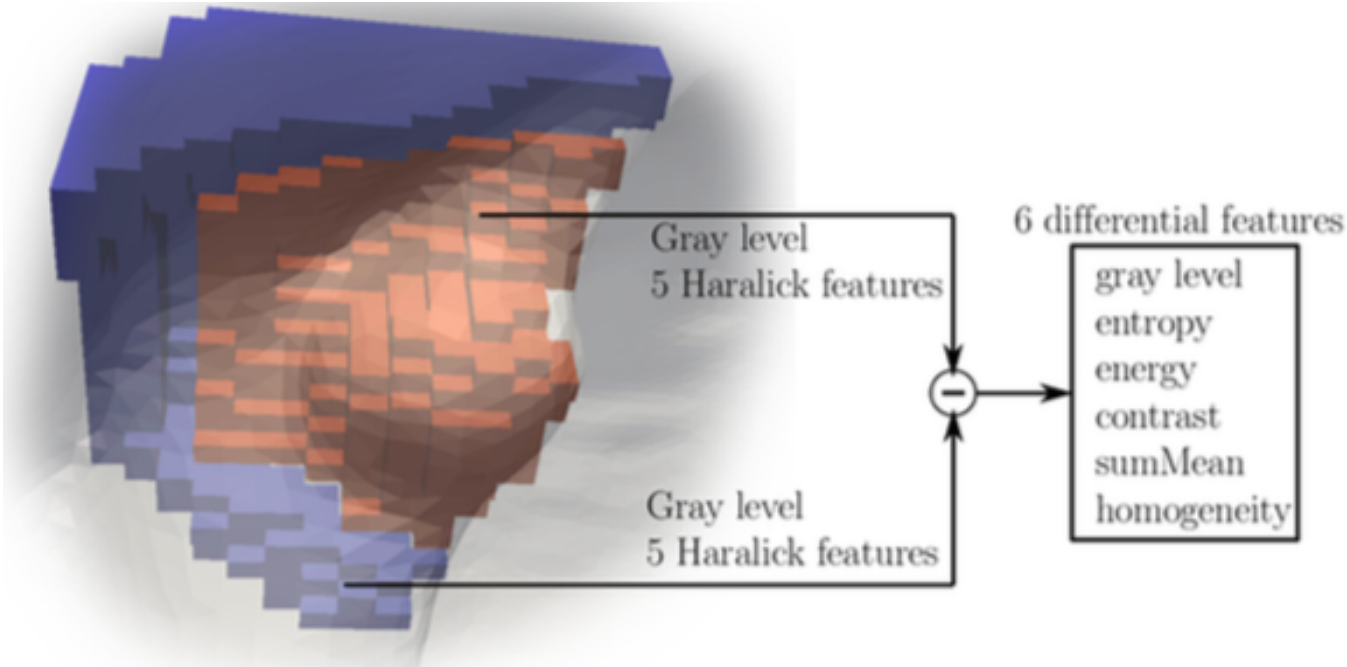

Final methodological remarks (1)

- **The final smoothing evolution equation becomes**

$$\frac{\partial \mathcal{S}}{\partial t} = g(SI)\, \kappa_{min}^{1/4} \vec{\mathcal{N}},$$

where $g(SI) = \frac{1}{\pi} \arctan\left((SI - 0.75) \cdot 10\right) + \frac{1}{2}$. This is a smooth function that assigns low values to SI near -1, and values close to unity to other points.

- This motion keeps all the advantages of the motion by $\kappa_{min}^{1/4}$ and in addition, polyps are flattened more slowly, so at the end the obtained surface is smooth and the polyps still stand out.

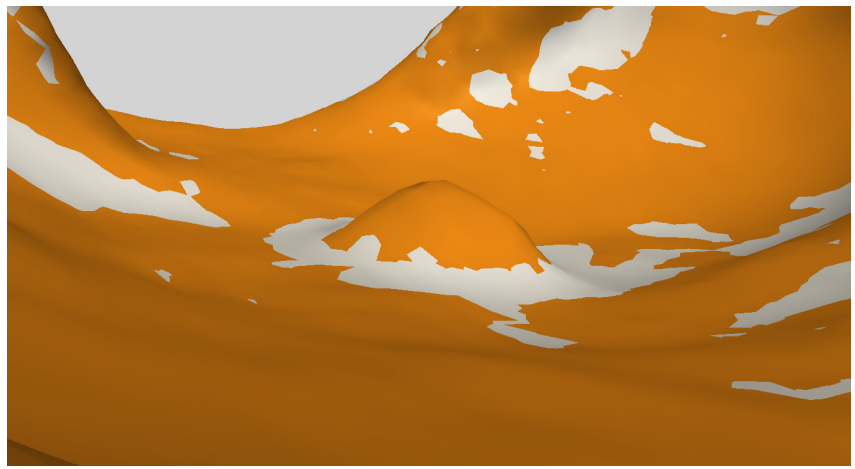

Comparison between evolutions. Motion by k_{min} in light gray vs. motion by $k_{min}^{1/4}$ in orange. Both surfaces are overlaid, so invisible sections are the other surface.

Final methodological remarks (2)

Candidate polyps delineation is performed by choosing, among a set of candidates centered at each x_0 with different patch and corresponding ring sizes, the ones that maximace the distance between their SI patch-ring histogram distance.

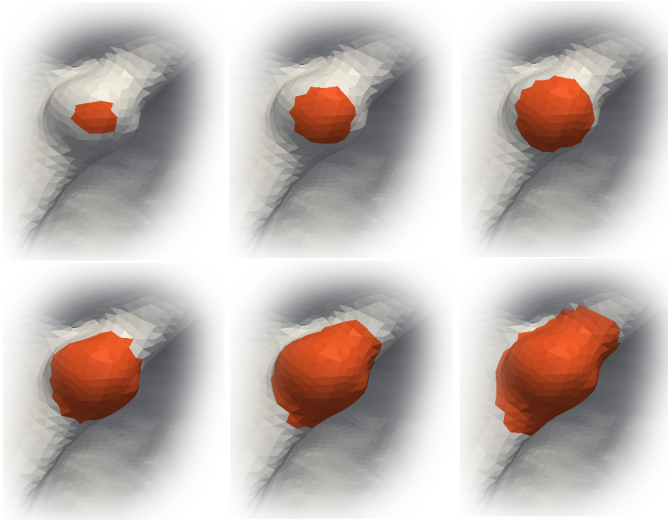

(a) Sets $\mathcal{P}_1 \ldots \mathcal{P}_n$: different sizes are tested in order to select the most appropriate patch.

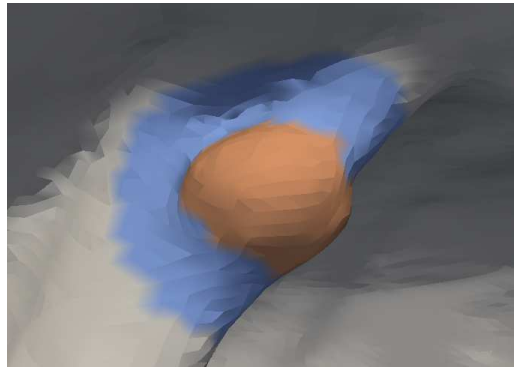

(b) Ring (in blue) surrounding a candidate polyp (in orange).

Patch size selection and ring around polyp.

Results (1): Performance by polyp size

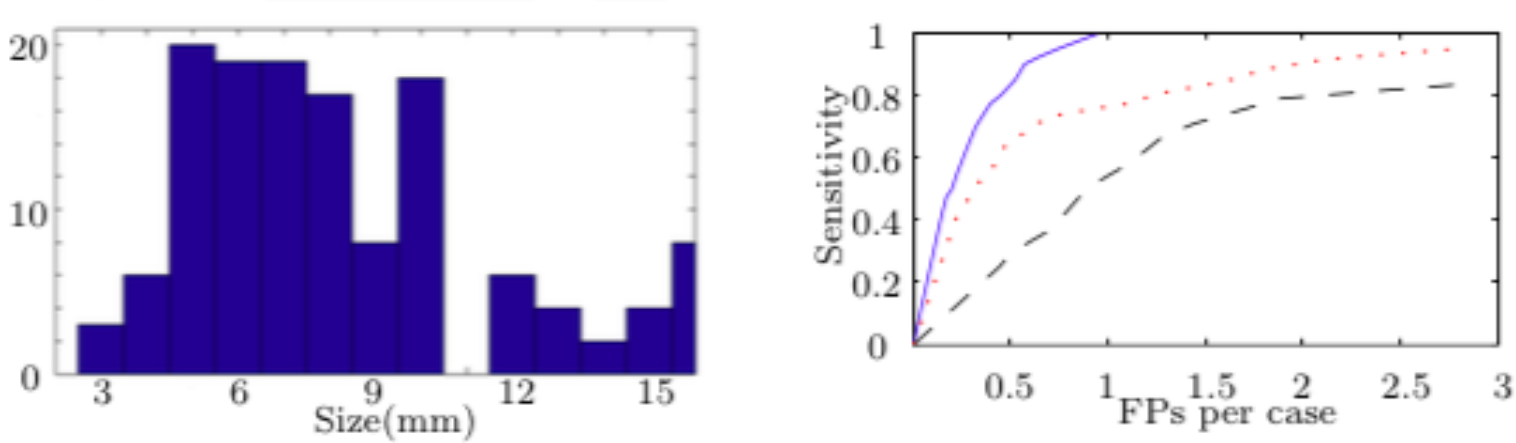

Fig. 9. Histogram of the polyps' sizes (left) and FROC curve of the proposed system for different polyps sizes: larger than $6mm$ (solid), smaller than $6mm$ (dashed), and all polyps (dotted).

Results (2): Influence of the smoothing PDE

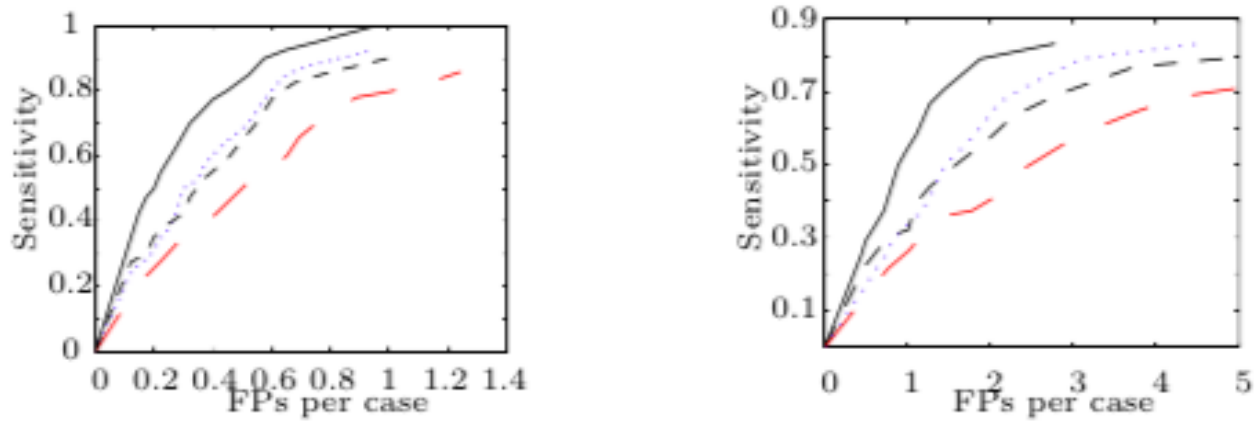

Fig. 10. FROC curve comparing the performances using the different smoothing methods, classifying large polyps (left) and small polyps (right). The curve for the proposed evolution is shown in solid line, the results for the evolution by $\mathcal{H}$ and κ_{min} are shown in dotted and dashed lines respectively, and the lower curve is the result when no smoothing is performed.

Results (3): Differential vs. Non-differential features

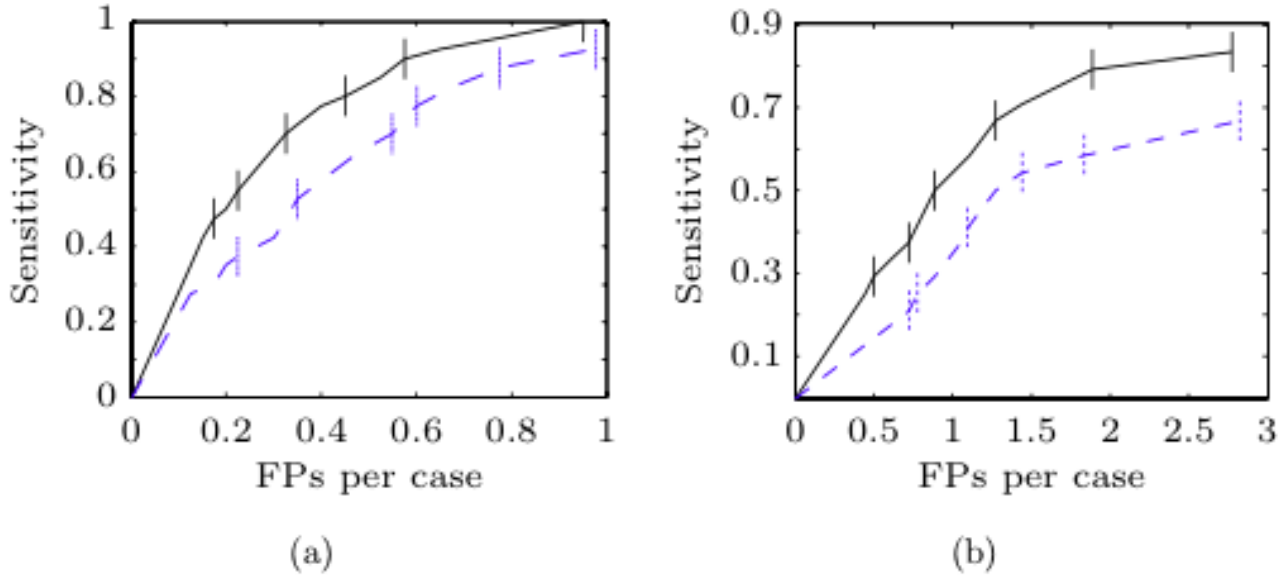

Fig. 10. FROC curve with 95% confidence intervals, comparing the performances with differential (solid) and absolute (dashed) texture features, classifying polyps larger than 6 mm in size (a) and smaller than 6 mm in size (b).

Results (4): Performance using different classifiers

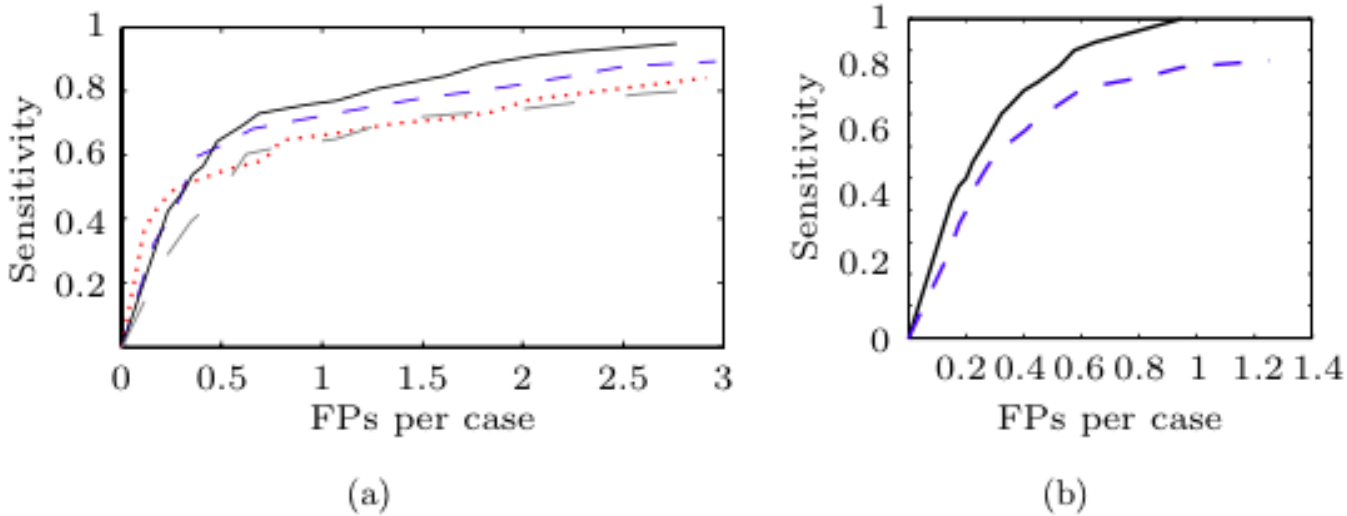

Fig. 11. (a) FROC curve comparing the performances of different classification approaches for all polyps. SVM with cost Sensitive (solid), SVM with SMOTE (dashed), C4.5 trees with AdaBoost (dotted) and plain SVM (long-dashed). (b) FROC curve of the final pipeline (solid) and without the IC computation (see Sec. 2.1).

Results (5): Geometric and texture importance

Table 1. Comparison of performance using only geometric versus only texture features.

	Features		
Polyps > 3 mm	All	Geometric	Texture
Sensitivity	93%	88%	68%
FPs p/case	2.8	6.5	19

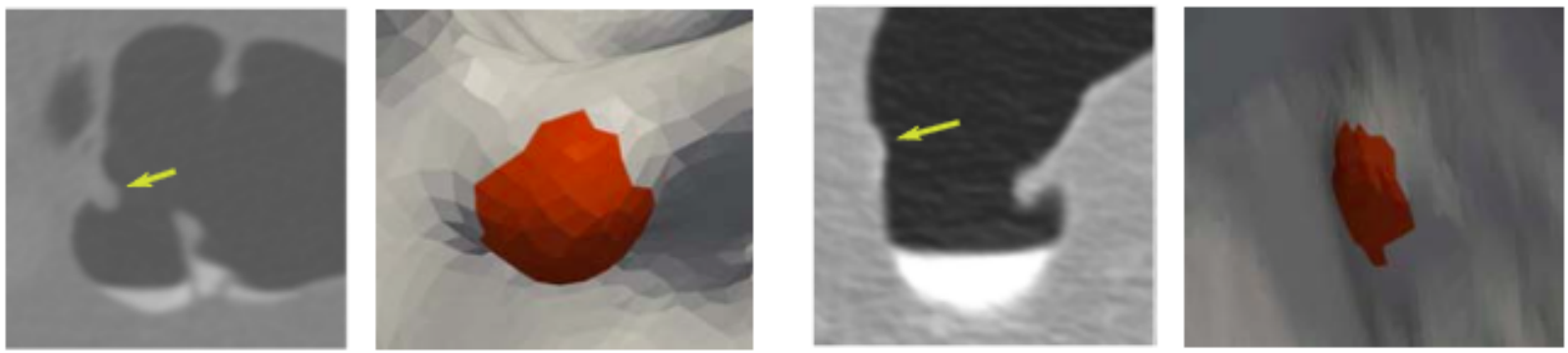

(a) (b)

Fig. 12. (a) Polyp with no texture information. (b) Polyp with texture information, but weak geometric information.

Results (6): Qualitative analysis of false positives

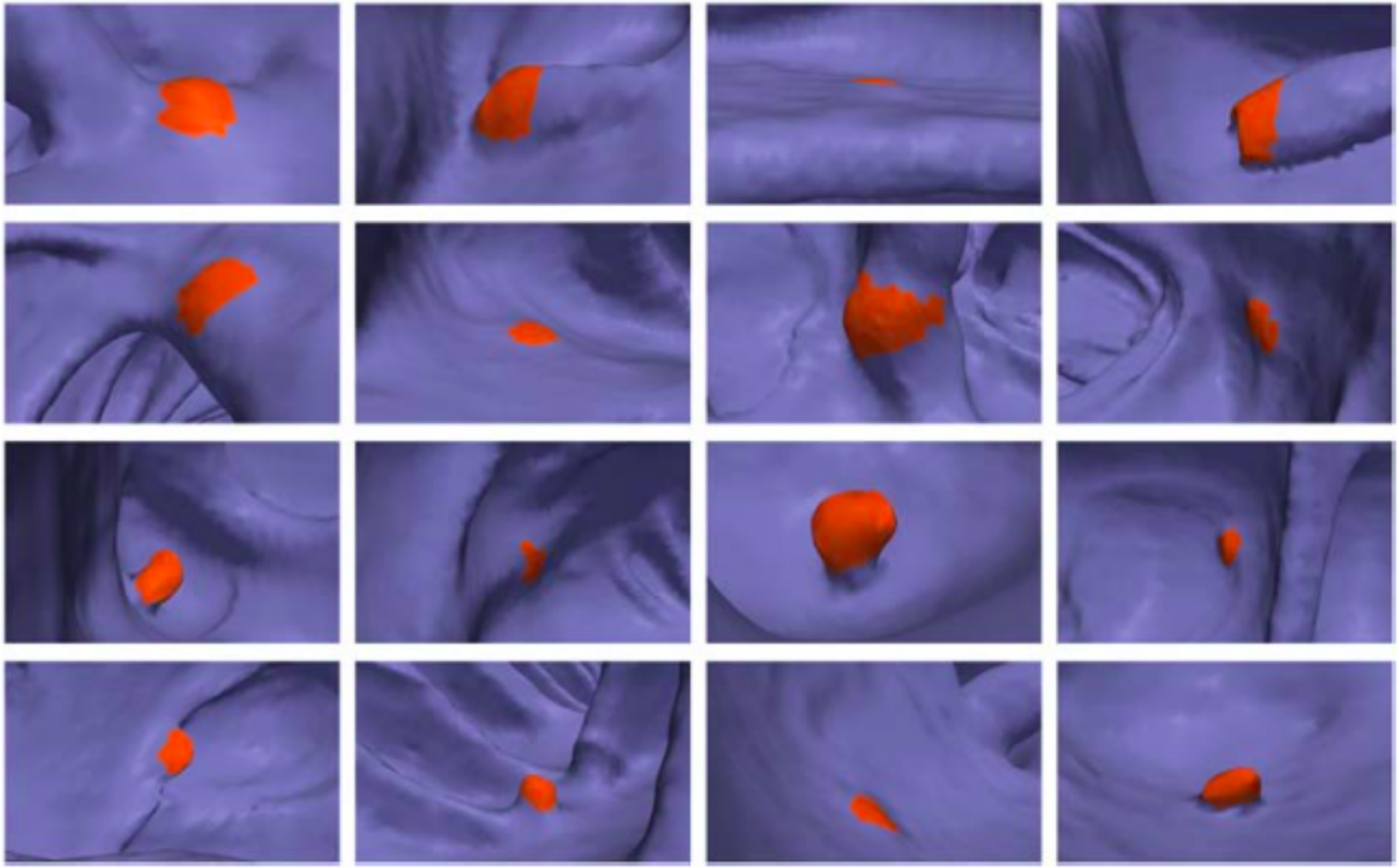

Fig. 14. Examples of false positives according to the available labeled data, with some segmentation errors, parts of the insufflation tube, and some patches with polyp-like shape.